Attractive Potential between Confined Colloids at Low Ionic Strength

Grace Martinelli Kepler* and Seth Fraden†
The Martin Fisher School of Physics, Brandeis University, Waltham, Massachusetts 02254
(Received 23 January 1994)

Digital video microscopy is used to locate the positions of 1.27 μm diameter polystyrene spheres suspended in low ionic strength water and confined between two glass plates. A method is developed to obtain the pair potential of the colloidal particles from measurements of the pair-correlation function of both dilute and moderately concentrated dispersions. We find that the measured pair potential has an attractive component much greater than predicted by the Derjaguin-Landau-Verwey-Overbeek theory of nonconfined colloids and suggest that the confining plates are responsible for the observed deviations from theory.

PACS numbers: 82.70.Dd, 05.40.+j, 61.25.Hq

The force and pair potential between charged colloids have been measured with a variety of techniques and systems. These include the force between charged mica cylinders of macroscopic size [1,2] and between 2 μm diameter polystyrene spheres [3]. Additionally, the potential of a single colloidal sphere confined between two charged glass plates has also been determined with several techniques [4,5]. In all of these cases, good agreement between theory and experiment has been obtained by treating the interparticle interaction as a balance between the electrostatic repulsion of the charged spheres and their associated counterions and the van der Waals attraction. This theoretical framework is known as the Derjaguin-Landau-Verwey-Overbeek (DLVO) potential [2,6,7]. However, none of the above techniques is suitable to determine the potential between colloids in confined geometries.

In this paper we report on a technique to determine the pair potential between colloidal particles in a confined geometry, even for the case of a nondilute suspension. We use video microscopy to locate the positions of micron sized spheres in colloidal suspensions confined between two glass plates and directly determine the pair-correlation function $g(r)$ as a function of ionic strength. For sufficiently dilute dispersions the relationship

$$g(r) = \exp[-U(r)/k_BT] \quad (1)$$

can be used to directly obtain the pair potential [8]. At higher concentrations $U(r)$ will not be the true pair potential, but some larger effective potential that includes the pair potential and the effect of many-body correlations. For example, $g(r)$ of a hard-sphere system with no attractive pair potential will show a peak and eventually oscillations as the density is increased. To extract the true pair potential $U_p(r)$ from $U(r)$ we performed a Brownian dynamics simulation with the same particle density as the experiment using $U(r)$ as the pair potential. If $U(r)$ has a deeper minimum than $U_p(r)$ due to many-body interactions, it follows that the simulated pair-correlation function will have a maximum larger than the experimentally measured $g(r)$. We then reduce the minimum of $U(r)$ to obtain a trial pair potential $U_s(r)$ and repeat the simulation with $U_s(r)$ until the simulated and experimental $g(r)$ agree. At this point we identify $U_s(r)$ with the true pair potential $U_p(r)$.

The experimental confined-geometry sample cell consists of two parallel windows of 25 × 25 mm microscope slide glass. A small glass post (3 × 3 ×1.5 mm) is glued to the upper glass window with transparent optical adhesive, and the spacing of the plates is adjusted until the gap between the post and the lower glass window is sufficient to confine the motion of the spheres to a single plane. The colloidal particles were polystyrene spheres of 1.27 μm diameter, which have a negative surface charge ($\sim 0.1e/\text{nm}^2$) and are repelled by the negative charge of the glass plates ($\sim 0.5e/\text{nm}^2$) in water. This acts to confine the spheres to a plane midway between the glass plates. The gap is typically 2–6 μm depending upon the ionic concentration and is adjusted with the aid of a monochromatic light source, so that the fringes can be used to monitor parallelism [9]. We measured the fluctuations of the spheres out of the midplane to have a rms value between 0.06 and 0.16 μm [4]. The spheres were suspended in a density-matching 50:50 mixture of D_2O and H_2O. De-ionizing resin was present in some of the cells to reduce the ionic concentration, though none was present in the thin gap.

Because of the confined geometry, the ionic strength and density of spheres in the gap cannot be directly controlled. The relationship between the concentration of the bulk solution and the concentration of colloid in the gap is dependent on many variables, including the charge and spacing of the plates, and whether de-ionizing resin is in the cell since the colloid tends to stick to the cation exchange resin. The ionic strength of the colloidal dispersions is difficult to measure because of the small dimensions of the gap. In addition, the large surface area to volume ratio of the cells means that the ionic strength of any dispersion added to the cell may be different than the ionic strength within the cell due to ions leaching

0031-9007/94/73(2)/356(4)$06.00

from the glass surfaces.

The spheres were viewed with an inverted microscope, with a 40× objective and long working length condenser operated in transmission mode. Images were recorded on a time-lapse video tape recorder (typically 1.2 sec per field) using a charged coupled device camera mounted on the microscope. The error in the measurement of sphere separations for spheres in the same plane was measured to be 0.02 μm. In addition, the spheres have some small motion out of the plane and a resulting error in measurement of the (2D) sphere separations. In microscopy, we measure the projection of the sphere separations onto the image plane, so that out-of-plane fluctuations distort the true $g(r)$ leading to a softening of the repulsive part of the pair potential, as well as a shift of the minimum to smaller interparticle separations. However, for the magnitude of the out-of-plane fluctuations given above, the error in the sphere separation measurements is estimated to be 0.014 μm.

After video taping, digital image analysis provided the particle positions from which the pair-correlation function was calculated. For the results reported here, between 500 and 5000 images (90×70 μm) were processed for each data set, depending upon the density of the sample, which varied from $\sim$ 30 to 300 particles per image.

Figure 1 shows the experimentally obtained $g(r)$ data for different cells as a function of the normalized sphere separation, r/σ, where r is the center-to-center spacing of the spheres and σ is the sphere diameter. In all cases, there is only a single peak in $g(r)$ and no liquidlike oscillations. Since the spheres have identical charges they will repel each other at small separations. An effective diameter of the spheres can be defined as the separation at which the pair potential is equal to k_BT, and can be located in Fig. 1 [using Eq. (1)] as the distance where $g(r) = 1/e$. This effective diameter will increase as the

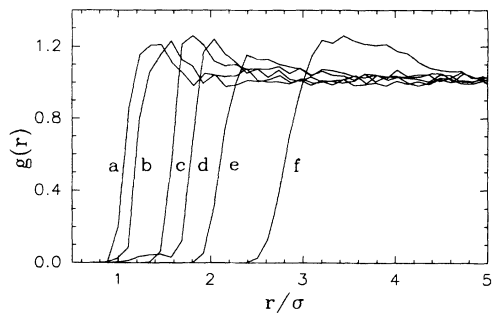

FIG. 1. Experimentally measured pair-correlation functions $g(r)$, for dilute suspensions of confined polystyrene spheres of diameter $\sigma = 1.27$ μm. The data shown here represent six different cells with decreasing ionic strength, as evidenced by the increase of the effective diameter [the distance where $g(r) = 1/e$]. Actual measurements of the ionic strength were not possible in the confined geometry. The number densities for the data were as follows: a, 5.8×10^{-3}; b, 21×10^{-3}; c, 12×10^{-3}; d, 24×10^{-3}; e, 15×10^{-3}; f, 19×10^{-3} μm^{-2}.

Debye screening length (κ^{-1}) increases, or as the ionic strength decreases.

The Brownian dynamics simulations used in the iterative procedure to extract the pair potential from $U(r)$ of Eq. (1) were carried out for 960 particles with positions updated according to the algorithm of Ermak [10]. Simulation conditions included wrap-around boundary conditions, a layered-cell method [11] for determining pairs of interacting particles, and a lookup table for pair forces. The lookup tables were generated from a piecewise fit of the initial $U(r)$ that were obtained from the experimental $g(r)$ of Fig. 1. The potentials were fit to a modified Lennard-Jones (LJ) potential, $U(r)/k_BT = 4\epsilon[(\mu/p)^{2a} - (\mu/p)^a]$, where $p = (r/\sigma) - 1$, σ is the sphere diameter, ϵ is the depth of the potential minimum, and μ and a are the fitted parameters. If the simulated $g(r)$ had a maximum greater than the experimental, then the parameter ϵ governing the potential minimum was reduced producing a new trial pair potential $U_s(r)$ for the next iteration of the simulation.

This iterative procedure was tested in two ways. First, a simulation was performed using a known Lennard-Jones pair potential with $\epsilon = 0.2$, which is similar to the potential derived directly through Eq. (1) from the data of Fig. 1 curve a, but at a higher particle density of 63×10^{-3} μm^{-2}, where many-body interactions begin to contribute to $g(r)$. Using the simulated $g(r)$, an effective potential was directly obtained through Eq. (1). This effective potential showed a deeper minimum than the pair potential with $\epsilon = 0.3$ due to the many-body interactions, and when this effective potential was used to perform a second simulation, the resulting $g(r)$ had a maximum greater than the first simulated $g(r)$. After several iterations of reducing ϵ, the simulated $g(r)$ agreed with the test $g(r)$. The pair potential that was extracted from the effective potential had slight systematic deviations from the true pair potential. The position of the potential minimum was underestimated by 12%, while the depth of the minimum was determined within 5%. The deviations arise for Lennard-Jones particles because an increase in particle density will cause the $g(r)$ peak to shift towards smaller sphere separations. Thus the derived potential will tend to underestimate the sphere separation corresponding to the potential minimum. From the results of this test, we conclude that the iterative procedure is reasonable for densities that are not too far from dilute.

A second test of the iterative procedure used the pair-correlation data of Fig. 2 obtained with two cells of roughly the same ionic strength, with the lower density data corresponding to the data in Fig. 1, curve a. Despite almost an order of magnitude difference in density between the two cells (5.6×10^{-3} and 52×10^{-3} μm^{-2}), the peak in $g(r)$ remains essentially the same. The fact that $g(r)$ is not changed by a significant increase in density would indicate that the peak in $g(r)$ is not the result of many-body correlations, but rather arises from an at-

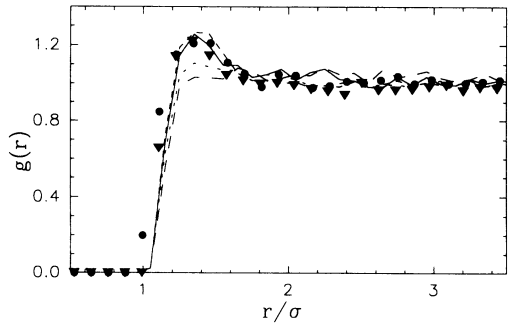

FIG. 2. Comparison of the pair correlation $g(r)$ for two different cells with the same ionic strength, but different densities: (solid circle) 5.8×10^{-3} and (triangle) 52×10^{-3} μm^{-2}. Also shown are the $g(r)$ obtained from computer simulations: (solid line) 5.8×10^{-3} and (dashed line) 52×10^{-3} μm^{-2}. The pair potentials used in the simulations were obtained directly from Eq. (1). Both the experimental and simulation data show that $g(r)$ is density independent, despite almost an order of magnitude difference in density. Also shown are $g(r)$ curves from simulations using a WCA potential consisting of only the repulsive component of the pair potential: (long dashed line) 5.8×10^{-3} and (short dashed line) 52×10^{-3} μm^{-2}.

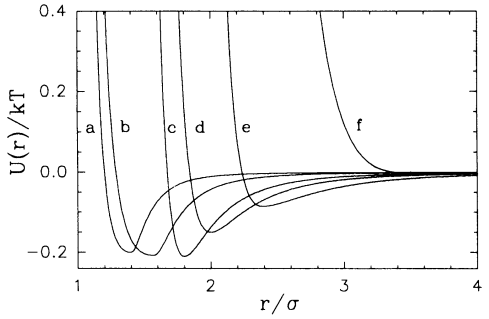

FIG. 3. The pair potential $U(r)$ per thermal energy k_BT as a function of sphere separation r per sphere diameter σ obtained from the pair-correlation data of Fig. 1. The pair potentials shown in a and b were obtained directly from Eq. (1) and the experimental $g(r)$. The pair potentials in curves c–f were obtained using the iterative simulation technique, with starting potentials obtained through direct inversion of the experimental $g(r)$ according to Eq. (1). Initially as the ionic strength decreases, the depth of the shallow minimum remains fairly constant even as the position of the minimum moves towards larger sphere separations. Eventually as the sphere separation increases, the depth of the minimum decreases, until it completely vanishes (curve f).

tractive pair potential. Thus the relationship in Eq. (1) can be used to obtain the pair potential directly.

Computer simulations using the data in Fig. 2 corroborate the suggestion that the peak in $g(r)$ arises exclusively from an attractive potential. The pair potential used in the simulations was obtained using the more dilute $g(r)$ data in that figure. Simulated $g(r)$ at the lower density showed good agreement with the experimental curves without the need to reduce ϵ. As a further check, a constant was added to the LJ potential to set the minimum to zero and the potential was also set to zero for all greater distances. This procedure is used to separate out the purely repulsive component of the interparticle forces, in the manner of Weeks, Chandler, and Anderson (WCA) [12]. The $g(r)$ that resulted from simulations with this repulsive interaction is also shown in Fig. 2. The fact that the peak in $g(r)$ disappears indicates that the peak is the result of the attractive component of the potential and is not caused by many-body correlations. Simulated $g(r)$ at the higher density also show good agreement with experiment without the need of iteration, though the $g(r)$ peak may be slightly increasing. Simulations at the higher density with the purely repulsive WCA potential show a small peak in $g(r)$.

Figure 3 shows the final pair potentials obtained from the data of Fig. 1 using the iterative procedure. For the first two data sets (a, b) with the greatest ionic concentrations, the dilute approximation was valid and the initial $U(r)$ obtained directly from $g(r)$ using Eq. (1) needed no modification in order to obtain good agreement between the experimental and simulated $g(r)$ curves. The original pair potential for the third data set (c) needed only a slight adjustment; the depth of the minimum, ϵ, was reduced by a factor of 0.91. For all three cases, simulations with only the repulsive component of the pair interaction resulted in $g(r)$ curves with no significant peaks, indicating that the peak in the experimental data is entirely accounted for by the attractive component of the interaction.

The three data sets with the lowest ionic concentrations (d–f) all needed substantial adjustment of the potential minima. Simulations with only the repulsive components of the pair interactions show an increasing peak in $g(r)$ as the ionic strength decreases. For data set f, with the lowest ionic concentration, the entire experimentally observed peak in $g(r)$ appears to be a result of many-body correlations of spheres interacting through a purely repulsive pair potential. Though the density is fairly constant among the samples, the dilute approximation is becoming less valid as the ionic strength decreases. This is reasonable since the effective diameter and effective density of the spheres increases as the screening length increases.

The pair potentials of Fig. 3 show a shallow potential minimum of approximately $0.2k_BT$ at a sphere separation of 1.4σ, which remains fairly constant up to a sphere separation of 1.8σ. For greater separations the attractive potential decays to zero.

We made a quantitative comparison of the final potentials with the DLVO potential for charged spheres in a *nonconfined* space because at present no theories are available that account for the influence of the highly charged glass plates on the sphere pair potential. We fitted the experimentally measured potentials to the fol-

lowing form [7]:

$$V_A = \frac{A}{12}\left[\frac{1}{x^2-1}+\frac{1}{x^2}+2\ln\left(\frac{x^2-1}{x^2}\right)\right],$$

$$V_R = \pi\epsilon\epsilon_0\sigma\Phi_0^2\,\frac{\exp[-\kappa\sigma(x-1)]}{x}, \qquad (2)$$

where V_A and V_R are, respectively, the attractive and repulsive components of the potential, A is the Hamaker constant, σ the particle diameter, Φ_0 the surface potential (fixed at 25 mV), and $x = r/\sigma$. These equations are valid for the case of $\kappa\sigma$ large. The fits were weighted to emphasize the depth, location, and width of the minimum of the pair-potential well.

With the surface potential fixed, the position and depth of the potential minimum are used to solve Eq. (2) for the Hamaker constant and Debye screening length (κ^{-1}) [13]. The fitted values of the Debye screening length (0.062, 0.093, 0.14, 0.17, and 0.23 μm) and Hamaker constant (1.1×10^{-19}, 3.4×10^{-19}, 11×10^{-19}, 16×10^{-19}, 33×10^{-19} J) for the data sets (a–e) of Fig. 3 increased as the ionic strength decreased, as one would expect [15]. However, the fitted Hamaker constants are several orders of magnitude larger than previous measurements [3] and theoretical calculations [15], which put it in the range of 10^{-21} to 10^{-20} J . We also fitted the data by Eq. (2) using a higher surface potential (100 mV) and used the constant charge boundary condition instead of constant voltage [2,7], but the same conclusion was always reached: The fitted Hamaker constants are orders of magnitude too large. Alternatively, we fixed the Hamaker constant in the range of 10^{-20} J and let the other parameters vary, but this resulted in too small values of the surface potential ($\sim$ 5 mV) and predicts rapid aggregation of the colloids, in contradiction with observation. This leads us to the conclusion that the DLVO potential for nonconfined colloids is inapplicable to the case of colloids confined by charged plates.

In this paper video microscopy techniques were used to directly measure the pair-correlation function $g(r)$ for dilute colloidal suspensions in a confined geometry. This results in a model independent method of deducing the effective interparticle potential $U(r)$. Using the Boltzmann expression [Eq. (1)] and Brownian dynamics simulations, the sphere pair potential was obtained over a wide range of sphere interaction lengths. The experimentally measured potential could be made to fit a DLVO potential only by using Hamaker constants much greater than the literature values. We do not interpret this to imply that the Hamaker constants are enhanced by the presence of the plates, or to imply a failure of the DLVO theory, especially in light of the agreement between the DLVO theory and experiment for nonconfined objects discussed in the first paragraph of this Letter. Rather, we speculate that the origin of the measured attractive pair potential of Fig. 3 arises from the electrostatic influence of the confining glass plates and suggest the need for theoretical work to investigate this possibility.

We acknowledge R. B. Meyer for his constant support and participation in this project. This research was supported by NSF DMR–459850 and DOE DE–FG02–87ER45084.

* Current address: CIIT, P.O. Box 12137, Research Triangle Park, NC 27709.
† To whom correspondence should be addressed.

[1] J.N. Israelachvili and G.E. Adams, J. Chem. Soc. Faraday Trans. I **74**, 975 (1978).
[2] J. Israelachvili, *Intermolecular and Surface Forces* (Academic, New York, 1991) 2nd ed.
[3] Y.Q. Li, N.J. Tao, J. Pan, A.A. Garcia, and S.M. Lindsay, Langmuir **9**, 637 (1993).
[4] G.M. Kepler and S. Fraden (to be published).
[5] D.C. Prieve and N.A. Frej, Langmuir **6**, 396 (1990); M.A. Brown and E.J. Staples, Langmuir **6**, 1260 (1990).
[6] E.J. Verwey and J.TH.G. Overbeek, *Theory of the Stability of Lyophobic Colloids* (Elsevier, New York, 1948).
[7] W.B. Russel, D.A. Saville, and W.R. Schowalter, *Colloidal Dispersions* (Cambridge University Press, Cambrdige, 1989).
[8] D.A. McQuarrie, *Statistical Mechanics* (Harper & Row, New York, 1973).
[9] A. Hurd, Ph.D. thesis, University of Colorado, Boulder, 1981.
[10] D.L. Ermak, J. Chem. Phys. **62**, 4189 (1975).
[11] D.C. Rappaport, in *Computer Modeling of Fluids, Polymers, and Solids*, edited by C.R. Catlow, S.C. Parker, and M.P. Allen (Kluwer Academic, Dordrecht, 1990).
[12] J.D. Weeks, D. Chandler, and H.C. Anderson, J. Chem. Phys. **54**, 5237 (1971).
[13] Alternatively an effective charge [14], or surface potential, for the colloids of data set f was found by letting $\Phi_0 = Z^*e/2\pi\epsilon\epsilon_0\sigma$ in Eq. (2) and fitting for both $C = 2\lambda_B Z^*/\sigma$, with λ_B the bjerrum length, and κ^{-1}. The fitted values were $\kappa^{-1} = 0.21$ μm and $C = 14$.
[14] S. Alexander, P.M. Chaikin, P. Grant, G.J. Morales, P. Pincus, and D. Hone, J. Chem. Phys. **80**, 5776 (1984).
[15] R. Evans and D.H. Napper, J. Colloid Interface Sci. **45**, 138 (1973); V.A. Parsegian, *Physical Chemistry: Enriching Topics From Colloid and Interface Science*, edited by H. van Olphen and K.J. Mysels (IUPAC, CA, 1975); R. Buscall and R.H. Ottewill, *Polymer Colloids*, edited by R. Buscall *et al.* (Elsevier, New York, 1985).